# Accepted Manuscript


Oxazoline as acceptor moiety for excited-state intramolecular proton transfer

Joel S. Reis, Arthur B. Fernandes, Barbara C. Freitas-Dörr, Erick L. Bastos, Hélio A. Stefani

PII: S0040-4020(18)31213-4

DOI: 10.1016/j.tet.2018.10.019

Reference: TET 29852

To appear in: *Tetrahedron*

Received Date: 31 August 2018

Revised Date: 9 October 2018

Accepted Date: 10 October 2018

Please cite this article as: Reis JS, Fernandes AB, Freitas-Dörr BC, Bastos EL, Stefani HéA, Oxazoline as acceptor moiety for excited-state intramolecular proton transfer, *Tetrahedron* (2018), doi: https://doi.org/10.1016/j.tet.2018.10.019.

**ARTICLE**

# Oxazoline as acceptor moiety for excited-state intramolecular proton transfer

Joel S. Reis[a,‡], Arthur B. Fernandes[b,‡], Barbara C. Freitas-Dörr[b,‡], Erick L. Bastos[*,b] and Hélio A. Stefani[*,a]

[a]Departamento de Farmácia, Faculdade de Ciências Farmacêuticas, Universidade de São Paulo, São Paulo, SP, Brazil.

[b]Departamento de Química Fundamental, Instituto de Química, Universidade de São Paulo, São Paulo, SP, Brazil.

[‡]These authors contributed equally to this work.

[*]Corresponding authors: elbastos@iq.usp.br; hstefani@usp.br.

## ABSTRACT

Excited state intramolecular proton transfer (ESIPT) is a widespread phenomenon that has been exploited in several analytical and technological applications. Here we describe the synthesis of two ESIPT-active halogen-substituted naphthol-oxazolines that can be conveniently functionalized to develop tailored sensors, and a *bis*-oxazoline that showcases the potential of oxazolines to undergo double ESIPT. The photophysical properties of these compounds in solution were investigated using polar aprotic solvents and the results were rationalized using DFT/TD-DFT calculations.


**Keywords** – oxazoline, fluorescence, ESIPT, ESIDPT, phototautomerization, solvent effects.

## GRAPHICAL ABSTRACT

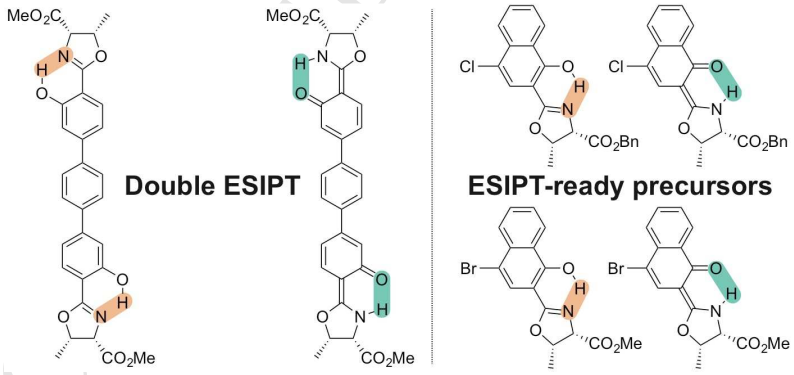

## 1. INTRODUCTION

Excited-state intramolecular proton transfer (ESIPT) is a common process in nature that has several applications such as bioimaging probes, chemosensors, molecular switches, organic light-emitting devices, and laser dyes.[1] ESIPT requires a preformed intramolecular hydrogen bond between photoacidic and photobasic groups. Upon photoexcitation, charge redistribution leads to fast adiabatic proton transfer along the excited state potential energy surface, resulting in tautomeric transformation.[2–4]

Photoexcitation can produce more than one electronically excited tautomer, which eventually decays to the ground state by fluorescence.[5,6] The maximum emission wavelength of the ESIPT tautomer is red-shifted with respect to the emission of the other tautomer, *i.e.* has Stokes' shift between 6,000 – 12,000 $cm^{-1}$, preventing self-reabsorption.[7] ESIPT dynamics depends on factors affecting hydrogen bond formation, such as molecular structure, temperature, and solvent. Control of the intrinsic and extrinsic properties of ESIPT systems led to the development of multi-emissive materials. For example, excited state intramolecular double proton transfer, viz., ESIDPT or double ESIPT, was used to generate multiple fluorescent intermediates.[3,4]

The type of proton donor and proton acceptor is fundamental to hinder or promote the ESIPT process.[1,3,8,9] Phenols and naphthols are common photoacids in ESIPT-active molecules because their acid dissociation constants are much higher in the ground state than in the excited state ($pK_a^* < pK_a$).[10] Additionally, the potential barrier for the occurrence of ESIPT from O–H type donors is often very small.[8] Heterocyclic compounds, such as benzothiazoles, benzimidazoles, and benzazoles, are typical ESIPT acceptors.[8,11] However,

the search for alternative ESIPT-active systems has led to new emitters, which have been used in myriad applications.[4,12]

Oxazolines are heterocyclic compounds found in many bioactive natural products[13–17] and drugs, including anti-inflammatory, anti-HIV, and antitumor agents.[18–20] The oxazoline ring has low reactivity towards nucleophiles, radicals, oxidizing agents, and acids, being used in applications requiring high chemical resistance.[21,22] Examples include oxazolinic linkers in asymmetric catalysis,[23] monomeric building blocks,[24,25] and ligands in cross-coupling reactions[26–30]. Fluorescent oxazolines are stable ligands for biosensing applications[31–36] and ESIPT-active oxazolines were used as synthons for photoinduced intramolecular cycloaddition reactions.[37,38] Therefore, the development of functionalizable ESIPT-active oxazolines can lead to versatile functional compounds, including sensors.

Here we demonstrate the potential of oxazolines as proton acceptors for the development of ESIPT-active molecules. Two ESIPT-active halogenated 1-naphthol oxazolines and a potential ESIDPT system based on a twisted bis(*o*-phenol oxazoline) were synthesized by using thionyl halide-promoted cyclization of aryl amides[39], and the occurrence of ESIPT was investigated in several polar aprotic solvents. The results were rationalized using DFT/TD-DFT calculations.

## 2. EXPERIMENTAL DETAILS

### 2.1 General

Starting materials were purchased from commercial sources and used without further purification. Solvents were purified and dried immediately before use. Melting points were measured using a Buchi B-545 apparatus. FTIR spectra were registered using a Agilent Cary 630 spectrophotometer. $^{1}H$ and $^{13}C$ NMR spectra were recorded on a Bruker DPX 300 at 300 MHz and 75 MHz, respectively. Chemical shifts (δ) are reported in ppm, referenced to the solvent signal of $CDCl_3$ or tetramethylsilane (TMS) and coupling constants (*J*) are reported in Hz. High-Resolution Mass Spectra were obtained using a Shimadzu LCMS-IT-TOF mass spectrometer. Absorption spectra were recorded using a Varian Cary 50 Bio spectrophotometer. Fluorescence excitation and emission spectra were acquired using a Varian Cary Eclipse spectrometer using quartz cells (optical path length: 10 mm) at 25 ± 1 °C.

### 2.2 Synthesis

The following section describes the last step of the synthesis of **1**–**3**. The complete description of the syntheses and the characterization ($^{1}H$ and $^{13}C$ NMR) of all intermediates and products is presented in the *Supporting Information (SI)*.

#### 2.2.1 Dimethyl 2,2'-(3,3''-dihydroxy-[1,1':4',1''-terphenyl]-4,4''-diyl)(4S,4'S,5S,5'S)-bis(5-methyl-4,5-dihydrooxazole-4-carboxylate) (1)

A stainless steel reactor was loaded with compound **9** (0.38 mmol, 273 mg), Pd/C 10 wt.% loading (20 mol%, 80 mg), MeOH (5 mL) and THF (5 mL). The system was closed and pressurized with $H_2$ (6 bar). The hydrogenolysis was carried out for 24 h at 25 ºC under magnetic stirring. Next, the pressure was slowly released and the reactor opened. The content was filtered off through a Celite pad, washing the pad with THF (5 × 5 mL). The volatiles were evaporated and the crude mixture was purified by chromatography column and eluted with hexane: EtOAc (3:2). Yield: 90%, white solid.

**m.p.** = 208-211 °C

**$^{1}$H NMR**: (300 MHz, $CDCl_3$): δ (ppm) 11.83 (bs, 1H), 7.75-7.68 (m, 3H), 7.34-7.25 (m, 1H), 7.21-7.15 (m, 1H), 5.13-5.00 (m, 2H), 3.80 (s, 3H), 1.45 (d, *J* = 5.7 Hz, 3H).

**$^{13}$C NMR**: (75 MHz, $CDCl_3$): δ (ppm) 169.8, 167.6, 160.6, 146.1, 139.9, 128.9, 127.8 (2C), 117.7, 115.3, 109.5, 70.5, 52.4, 16.2.

**$^{13}$C NMR APT**: (75 MHz, $CDCl_3$): δ (ppm) 169.8, 167.6, 160.5, 146.1, 139.8, 128.9, 127.7 (2C), 117.7, 115.2, 109.4, 77.5, 70.5, 52.3, 16.2.

**IR**: $\upsilon_{max}$ (neat, $cm^{-1}$) 2948, 1745, 1639, 1615, 1562, 1439, 1385, 1357, 1277, 1205, 1181, 1080, 1045, 812, 765.

**HRMS**: (ESI) *m/z*, calcd for [$C_{30}H_{28}N_2O_8 + H^+$]: 545.1924; found: 545.1932.

### 2.2.2 Benzyl (4S,5S)-2-(4-chloro-1-hydroxynaphthalen-2-yl)-5-methyl-4,5-dihydrooxazole-4-carboxylate (2)

In a 50-mL dry, two necked round bottom flask, under $N_2$ atmosphere was added the amide **11** (1.57 mmol, 597 mg), anhydrous DCM (15 mL) and $SOCl_2$ (40 equiv., 63 mmol, 4.6 mL). The reaction was stirred at 25 ºC until completion (48 h). The system was opened and

solid $Na_2CO_3$ was added in small portions (evolution of $CO_2$) until pH around 7 was reached, as indicated by indicator paper. The resulting suspension was filtered off through sintered glass funnel washing the pad with DCM (5 × 5 mL). The organic phase was dried under $MgSO_4$, filtered off and volatiles were evaporated. Yield: 85%, yellow solid

**m.p.** = 136-138 °C

**$^1$H NMR**: (300 MHz, $CDCl_3$): δ (ppm) 13.01 (bs, 1H), 8.45 (d, *J* = 8.2 Hz, 1H), 8.17 (d, *J* = 8.3 Hz, 1H), 7.75-7.65 (m, 2H), 7.62-7.55 (m, 1H), 7.40-7.30 (m, 5H), 5.23 (s, 2H), 5.12-5.03 (m, 2H), 1.37 (d, *J* = 5.5 Hz, 3H).

**$^{13}$C NMR**: (75 MHz, $CDCl_3$): δ (ppm) 169.1, 167.8, 158.3, 135.2, 133.4, 129.7, 128.8 (2C), 128.7, 126.4, 126.0, 124.4, 124.4, 123.2, 121.2, 103.3, 77.9, 70.2, 67.3, 16.1.

**IR**: $\upsilon_{max}$ (neat, $cm^{-1}$) 3032, 2983, 1734, 1631, 1598, 1501, 1458, 1408, 1374, 1352, 1290, 1238, 1222, 1190, 1145, 1088, 1048, 1030, 961, 905, 883, 847, 760, 750, 735, 698, 674.

**HRMS**: (ESI) *m/z*, calcd for $[C_{22}H_{18}ClNO_4 + H^+]$: 396.0997; found: 396.0996.

### 2.2.3 Methyl (4S,5S)-2-(4-bromo-1-hydroxynaphthalen-2-yl)-5-methyl-4,5-dihydrooxazole-4-carboxylate (3)

In a 50-mL dry, two necked round bottom flask, under $N_2$ atmosphere was added the amide **12** (1.55 mmol, 472 mg), anhydrous DCM (15 mL) and $SOBr_2$ (10 equiv., 15.5 mmol, 1.2 mL). The reaction was kept at 25 ºC and under stirring until the starting material was completely consumed (24 h) The work up was performed as described for compound **2**. Yield: 90%, purple solid

**m.p.** = 175-180 °C (decomp.)

**$^{1}$H NMR**: (300 MHz, $CDCl_3$): δ (ppm) 13.03 (s, 1H), 8.43 (d, *J* = 8.1 Hz, 1H), 8.14 (d, *J* = 8.4 Hz, 1H), 7.92 (s, 1H), 7.68 (t, *J* = 7.6 Hz, 1H), 7.56 (t, *J* = 7.5 Hz, 1H), 5.16 – 5.02 (m, 2H), 3.79 (s, 3H), 1.46 (d, *J* = 6.0 Hz, 3H).

**$^{13}$C NMR**: (75 MHz, $CDCl_3$): δ (ppm) 169.7, 167.6, 158.9, 134.5, 130.0, 127.1, 126.8, 126.4, 126.1, 124.4, 110.9, 104.1, 77.9, 70.2, 52.4, 16.2.

**IR**: $\upsilon_{max}$ (neat, $cm^{-1}$) 2957, 2928, 1749, 1631, 1601, 1505, 1460, 1410, 1380, 1357, 1244, 1225, 1203, 1153, 1100, 1089, 1046, 886, 802, 761.

**HRMS**: (ESI) *m/z*, calcd for [$C_{16}H_{14}BrNO_4 + H^+$]: 364.0184; found: 364.0157.

### 2.3 Fluorescence quantum yields

Fluorescence quantum yields ($\phi_{Fl}$) relative to the secondary standard were calculated using Eq. 1.

$$\phi_{Fl} = \phi_{Fl}^{r} \frac{A^r}{A} \frac{S}{S^r} \left( \frac{n_D}{n_D^r} \right)^2 \qquad \text{(Eq. 1)}$$

where the superscript *r* refers to the standard, *A* is the absorbance at the selected excitation wavelength, *S* is the area under the fluorescence emission curve and $n_D$ is the refraction index of the solvent. Quinine sulfate ($\phi_{Fl}^{r}$ = 0.546 in 0.1 mol $L^{-1}$ $H_2SO_4$, EX 300-360 nm; EM 400-600 nm) was used as secondary fluorescence standard. Samples were diluted to an absorbance lower than 0.1 at the excitation wavelength to avoid inner filter effects. Fluorescence spectra were recorded under the following experimental conditions: photomultiplier tension: 600 V; compound **1**, excitation wavelength ($\lambda_{ex}$): 330 nm, excitation and emission slits ($s_{ex}$, $s_{em}$): 5 nm and 10 nm, compounds **2** and **3**, $\lambda_{ex}$: 360 nm, $s_{ex}$, $s_{em}$: 10 nm.

### 2.4 Computational details

Ground state and first excited singlet state geometries were optimized without constraints at the DFT B3LYP/6-31+G(d,p) level.[40,41] Stationary points were characterized as minima by vibrational analysis. Linear optical properties were calculated using single point energy calculations at the TD-DFT SMD/B3LYP/6-31+G(d,p) level.[40,42] All calculations were carried out using the Gaussian 09 rev. D1 software package.[43] VMD was used to render all images of structures and surfaces.[44]

## 3. RESULTS AND DISCUSSION

### 3.1 Synthesis and characterization of 2-aryl oxazolines

Compound **1** was synthesized in six steps from 4-iodo-2-hydroxybenzoic acid (**4**) (Scheme 1). The double Suzuki-Miyaura cross-coupling between compound **5** and dipotassium phenylene-1,4-*bis*-trifluoroborate gives the triaryl adduct **6**. Following ester hydrolysis, amidation and $SOCl_2$-promoted cyclodehydration led to the desired compound **1** in 65% yield as a white solid. Oxazoline naphthoic derivatives **2** and **3** were synthesized in two steps from 1-hydroxy-2-naphthoic acid (**10**) and two different esters of L-threonine (Scheme 1). Precursor compounds **11** and **12** were obtained in moderate yields (52 and 48%) and were converted into products **2** and **3** in 85 and 90% yields, respectively, *via* combined cyclization and halogenation using thionyl halide.[39] These halogenated 1-naphthol oxazolines can be conveniently used as synthetic precursors of ESIPT-active sensors.

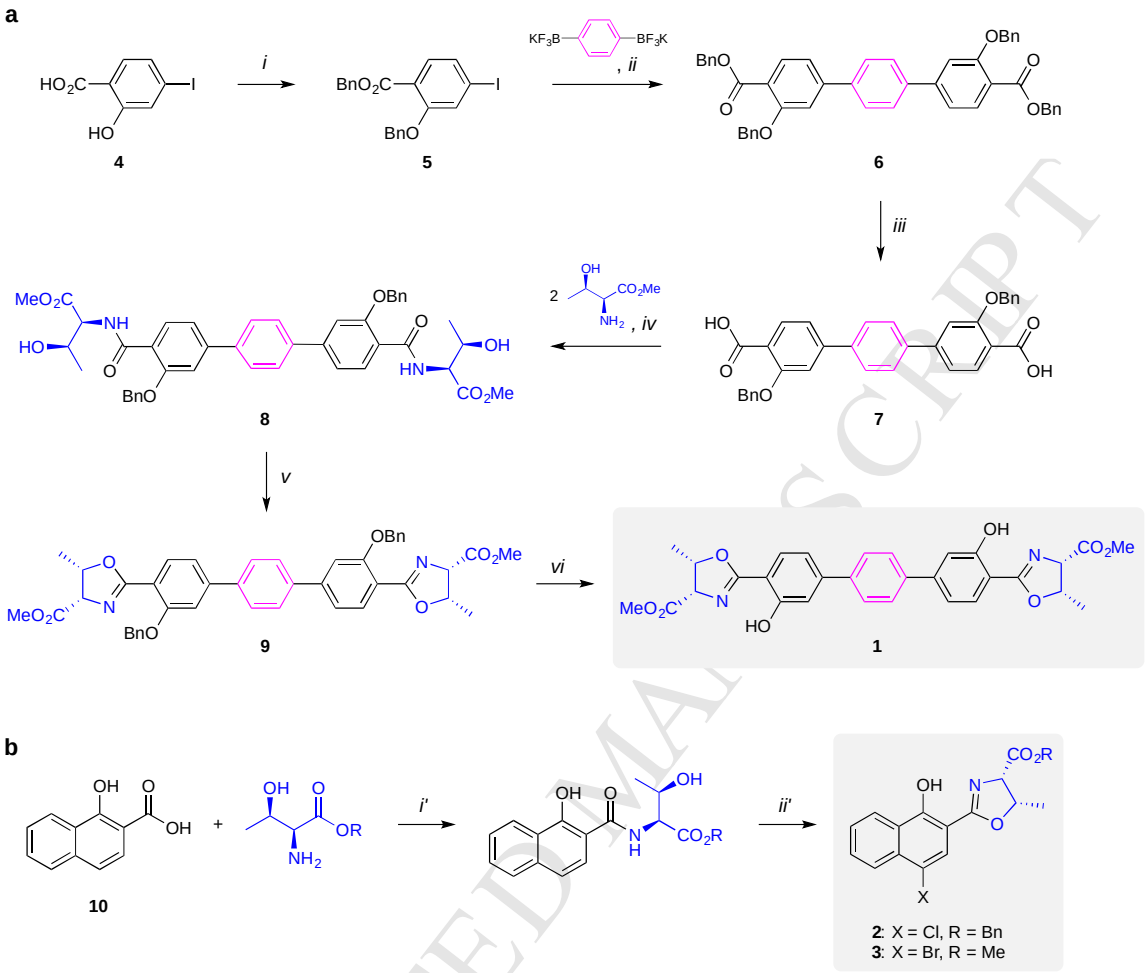


**Scheme 1.** Synthesis of the bis-oxazoline **1** (a) and the naphthoic oxazolines **2** and **3** (b). Reaction conditions: (a) *i*. BnBr, $K_2CO_3$, acetone, reflux, 24 h, 94%; *ii*. $Pd(dppf)Cl_2{\cdot}CH_2Cl_2$, $K_2CO_3$, THF:$H_2O$, reflux, 24 h, 87%; *iii*. NaOH aq. (1 mol $L^{-1}$), THF, reflux, 24 h, 99%; *iv*. EDC·HCl, 1-HOBt, NMM, DMF, 80 ºC, 24 h, 93%; *v*. $SOCl_2$, $CH_2Cl_2$, r.t., 5 h, $Na_2CO_3$, 95%; *vi*. $H_2$, Pd/C, THF:MeOH, r.t., 24 h, 91%; (b) *i'* (R = Bn). EDC·HCl, 1-HOBt, NMM, DCM, ultrasound, r.t., 2 h, 52%; *i'* (R = Me). EDC·HCl, 1-HOBt, NMM, DMF, r.t., 24 h, 48%; *ii'*. $SOCl_2$, $CH_2Cl_2$, r.t., 24-48 h, $Na_2CO_3$, 85-90%.

### 3.2 Photophysical properties of 2-aryloxazolines

Steady-state absorption and emission spectra of compounds **1**, **2** and **3** in polar aprotic solvents are shown in Figure 1; the derived photophysical parameters are compiled in Table 1. The solvent has minor influence on the absorption and fluorescence profiles of the *bis*-oxazoline **1**. For all solutions of compound **1**, absorption spectra show a major peak at around 330 nm (mean molar absorption coefficient is 33,000 L $mol^{-1}$ $cm^{-1}$) and a vibronic shoulder at roughly 290 nm. The fluorescence spectra of the *bis*-oxazoline **1** have a maximum at around 475 nm. The large Stokes shift (> 9,000 $cm^{-1}$, > 140 nm from 330 nm), characteristic of double ESIPT systems,[5,45,46] originates from the proton transfer (keto) tautomer of **1**. Dual emission is observed in acetone and DMSO, *i.e.*, at 400 nm and 475 nm, due to the presence of small amounts of the excited enol tautomer. The average fluorescence quantum yield is low ($\phi_{FL}$ around 10%), possibly due to vibrational deactivation of the singlet excited state.

The absorption spectra of naphthyl oxazoles **2** and **3** show the characteristic vibronic resolution of C2-substituted 1-naphthol compounds.[10,39,47] In DMF and DMSO, additional bands between 390 – 450 nm are observed. Data for **2** and **3** are similar since the the exchange of chlorine by bromine is not expected to affect the acidity of the naphthol group, *e.g.*, the p$K_a$s of 4-bromo-1-naphthol and 4-chloro-1-naphthol are 8.72 and 8.86, respectively.[48] Excitation of **2** and **3** at 360 nm results in broad emission bands with maxima at roughly 450 nm. Minor fluorescence solvatochromism is observed when DMSO and DMF are used as solvent. Excitation of solutions of **2** and **3** in DMSO or DMF at either 360 nm or 420 nm resulted in emission at 445 nm. The large Stokes shift observed (*ca.*

6,000 $cm^{-1}$) can be explained by the occurrence of ESIPT, resulting in emission from the excited keto tautomers of **2** and **3**. In all solvents, compound **3** presented much lower $\phi_{Fl}$ values compared to compound **2** (Table 1), probably due to the heavy atom effect of the bromine atom.[49–51] The nature of the ester group is not expected to affect the photophysical properties of naphthyl oxazoles **2** and **3**.[52,53]

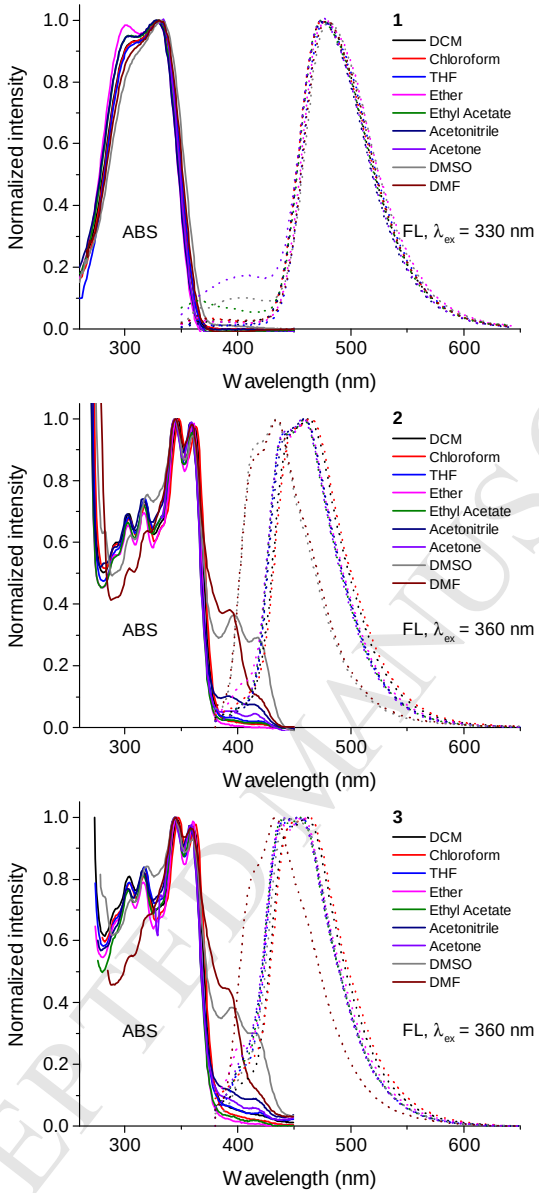


**Figure 1.** Normalized absorption and emission spectra of compounds **1**, **2**, and **3** in polar aprotic solvents at 25 ºC. [**1**]: 2 μmol $L^{-1}$, [**2**]: 30 μmol $L^{-1}$, and [**3**]: 30 μmol $L^{-1}$.

**Table 1.** Photophysical properties of compounds **1**–**3** in polar aprotic solvents.

| Solvent | $\lambda_{abs}$[a] | ε[b] | $\lambda_{EM}$[a] | Δυ[c] | $\Phi_F \times 10^2$ |
|---|---|---|---|---|---|

| | | | | | |
|---|---|---|---|---|---|
| | | | **1** | | |
| DCM | 330 | 39,000 | 475 | 9,250 | 6.6 |
| $CHCl_3$ | 330 | 41,000 | 474 | 9,210 | 9.6 |
| THF | 330 | 31,000 | 476 | 9,300 | 10.2 |
| $Et_2O$ | 327 | 29,000 | 477 | 9,620 | 9.4 |
| AcOEt | 329 | 31,000 | 475 | 9,340 | 6.1 |
| MeCN | 327 | 32,000 | 474 | 9,480 | 9.7 |
| Acetone | 333 | 31,000 | 475 | 8,980 | 6.1 |
| DMSO | 332 | 31,000 | 481 | 9,330 | 8.6 |
| DMF | 330 | 32,000 | 478 | 9,380 | 10.2 |
| | | | **2** | | |
| DCM | 360 | 5,200 | 462 | 6,130 | 3.5 |
| $CHCl_3$ | 362 | 4,800 | 465 | 6,120 | 3.1 |
| THF | 360 | 4,900 | 458 | 5,940 | 4.7 |
| $Et_2O$ | 361 | 5,000 | 459 | 5,910 | 2.4 |
| AcOEt | 359 | 4,500 | 459 | 6,070 | 4.5 |
| MeCN | 358 | 4,600 | 459 | 6,150 | 4.1 |
| Acetone | 358 | 4,800 | 459 | 6,150 | 4.8 |
| DMSO | 360 | 4,500 | 434 | 4,740 | 20.0 |
| DMF | 359 | 5,400 | 435 | 4,870 | 18.6 |
| | | | **3** | | |
| DCM | 360 | 4,500 | 461 | 6,090 | 0.8 |

| | | | | | |
|---|---|---|---|---|---|
| $CHCl_3$ | 362 | 4,300 | 464 | 6,070 | 0.8 |
| THF | 359 | 4,800 | 457 | 5,970 | 1.1 |
| $Et_2O$ | 359 | 3,800 | 457 | 5,970 | 0.6 |
| AcOEt | 359 | 3,800 | 455 | 5,880 | 1.1 |
| MeCN | 357 | 3,900 | 448 | 5,690 | 1.0 |
| Acetone | 359 | 4,100 | 454 | 5,830 | 0.8 |
| DMSO | 360 | 5,000 | 441 | 5,100 | 1.4 |
| DMF | 358 | 4,200 | 433 | 4,840 | 1.0 |

[a] in nm, [b] in (L $mol^{-1}$ $cm^{-1}$); determined by weight considering the Beer-Lambert relationship, [c] in $cm^{-1}$.

Geometry optimization of compounds **1**–**3** in the ground state indicates that the O–H···N hydrogen-bonded conformer is more stable than the O–H···O conformer, e.g., $\Delta_r G^0$ for isomerization of **2** is 20 kJ $mol^{-1}$. The tautomerization of compounds **1**–**3** is endergonic in the ground state (Figure 2a). For the *bis*-oxazoline **1**, single and double tautomerization have an energetic cost of 39 and 75 kJ $mol^{-1}$, respectively. However, considering the experimental energy for the $S_1 \rightarrow S_0$ transition, tautomerization is thermodynamically allowed on the singlet excited state potential surface. Results are similar for compounds **2** and **3**. Excitation of the bis-enol tautomer of compound **1** ($enol^2$) implies the initial formation of a locally excited (LE) state. Single and double ESIPT produce the keto-enol and the $keto^2$ tautomers, respectively, resulting in charge transfer towards the keto centers upon $S_1 \rightarrow S_0$ transition. Analysis of frontier orbitals involved in the excitation of **2** and **3** (Figure 2b) shows the nodal plane typical of C1/C2-substituted naphtalenes, *viz.*, the $^1L_a$

state ($\pi$-$\pi^*$, polarization along the short axis) of 1-naphthols is lower in energy than the $^1L_b$ state ($\pi$-$\pi^*$, polarization along the long axis).[53–55] Consequently, charge delocalization is not extended through the naphthalene ring; instead, functionalization of the ring by substitution of the halogen atom is expected to have a major influence on the electronic properties of the derivatives of **2** and **3**.

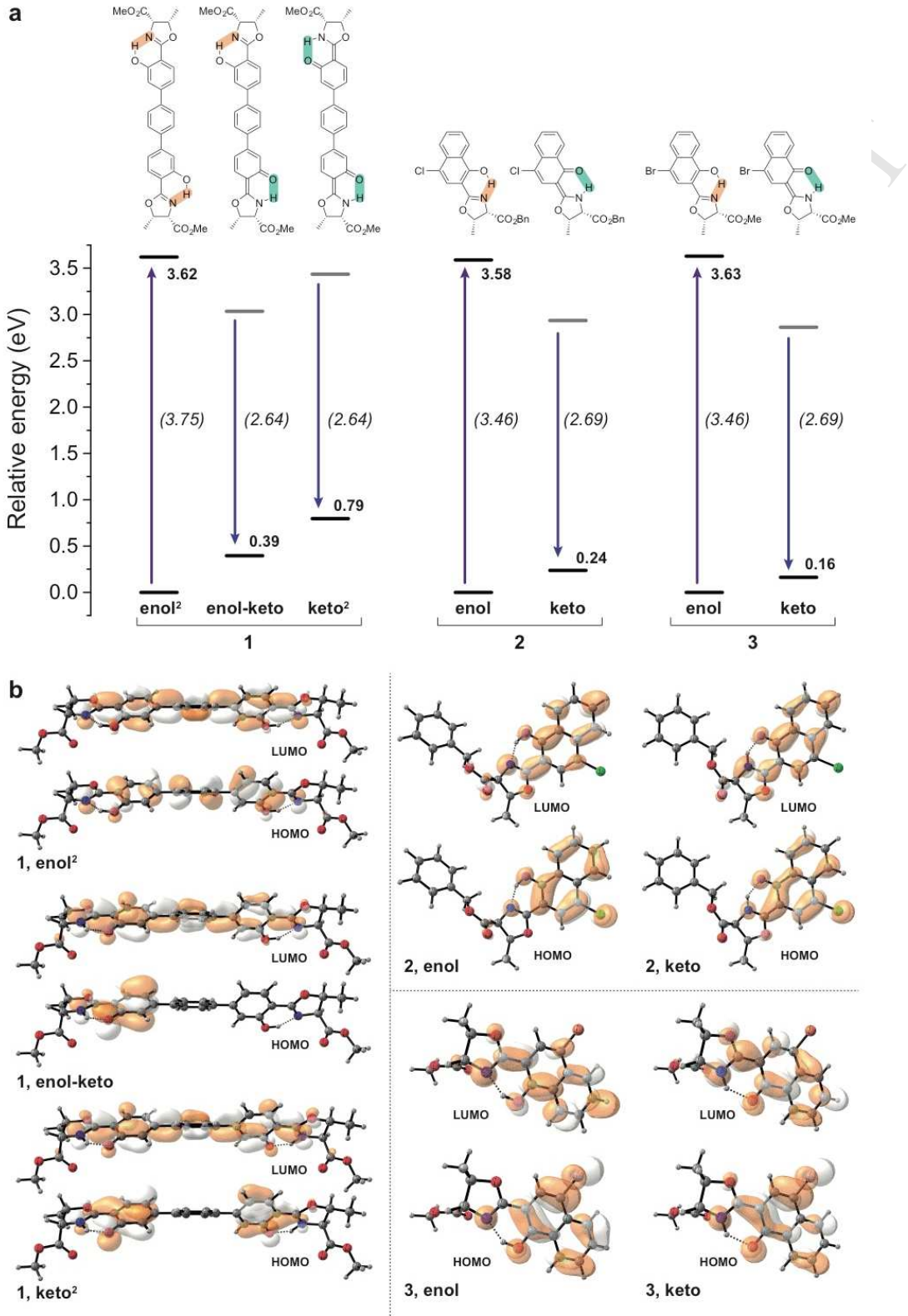
a
Relative energy (eV)
3.5
3.0
2.5
2.0
1.5
1.0
0.5
0.0
3.62
(3.75)
0.39
(2.64)
0.79
(2.64)
enol²
enol-keto
keto²
1
3.58
(3.46)
0.24
(2.69)
enol
keto
2
3.63
(3.46)
0.16
(2.69)
enol
keto
3
b
LUMO
HOMO
1, enol²
LUMO
HOMO
1, enol-keto
LUMO
HOMO
1, keto²
LUMO
HOMO
2, enol
LUMO
HOMO
2, keto
LUMO
HOMO
3, enol
LUMO
HOMO
3, keto

**Figure 2.** Electronic properties of oxazolines **1**–**3**. (a) Relative energies for electronic transitions involving the enol and keto tautomers. Numbers in parentheses correspond to the experimental data; the theoretical excitation energy and tautomerization energies are marked in bold. (b) Frontier molecular orbital relevant for the occurrence of ESIPT involving oxazolines **1**–**3**.

In conclusion, the use of thionyl halide-promoted cyclization of aryl amides allowed the synthesis of three prototype ESIPT-active 2-aryloxazolines. The *bis*-oxazoline **1** exhibits double ESIPT evidenced by a large Stokes shift and dual emission with fluorescence quantum yields of around 10%. Halogen-substituted oxazolines **2** and **3** show ESIPT in polar aprotic solvents. Fluorescence quantum yields are reduced by replacing the chlorine substituent by bromine, reinforcing the potential of these compounds to act as synthetic precursors of ESIPT-active sensors.

## ACKNOWLEDGEMENTS

This research was supported by FAPESP (grants J.S.R. 2016/02392-1; A.B.R. 2015/25629-4; B.C.F.D. 2014/10563-5; E.L.B. 2014/22136-4, 2016/21445-9; H.A.S. 2017/24821-4), and CNPq (E.L.B 303341/2016-5; H.A.S.-306119/2014-5).

## AUTHOR CONTRIBUTIONS

H.A.S. and E.L.B. proposed the concept and directed the research. J.S.R. conducted the synthesis; B.F.D. and A.B.R. acquired the absorption and fluorescence spectra and

analyzed the results. E.L.B. performed the theoretical calculations. All authors contributed to the writing and reviewing of the manuscript.

## ADDITIONAL INFORMATION

The authors declare no competing financial interests.

## 4. REFERENCES


1. Chen C-L, Chen Y-T, Demchenko AP, Chou P-T. Amino proton donors in excited-state intramolecular proton-transfer reactions. *Nat Rev Chem*. 2018;2(7):131-143. doi:10.1038/s41570-018-0020-z.
2. Mallick A, Purkayastha P, Chattopadhyay N. Photoprocesses of excited molecules in confined liquid environments: An overview. *J Photochem Photobiol C Photochem Rev*. 2007;8(3):109-127. doi:10.1016/j.jphotochemrev.2007.06.001.
3. Kwon JE, Park SY. Advanced organic optoelectronic materials: Harnessing excited-state intramolecular proton transfer (ESIPT) process. *Adv Mater*. 2011;23(32):3615-3642. doi:10.1002/adma.201102046.
4. Padalkar VS, Seki S. Excited-state intramolecular proton-transfer (ESIPT)-inspired solid state emitters. *Chem Soc Rev*. 2016;45(1):169-202. doi:10.1039/c5cs00543d.
5. Zhou P, Han K. Unraveling the Detailed Mechanism of Excited-State Proton Transfer. *Acc Chem Res*. 2018;51(7):1681-1690. doi:10.1021/acs.accounts.8b00172.
6. Massue J, Jacquemin D, Ulrich G. Molecular Engineering of Excited-State Intramolecular Proton Transfer (ESIPT) Dual and Triple Emitters. *Chem Lett*. 2018:cl.180495. doi:10.1246/cl.180495.
7. Xu L, Wang Q, Zhang Y. Electronic effect on the photophysical properties of 2-(2-hydroxyphenyl)benzothiazole-based excited state intramolecular proton transfer fluorophores synthesized by sonogashira-coupling reaction. *Dye Pigment*. 2017;136:732-741. doi:10.1016/j.dyepig.2016.09.024.
8. Kanlayakan N, Kerdpol K, Prommin C, et al. Effects of different proton donor and

acceptor groups on excited-state intramolecular proton transfers of amino-type and hydroxy-type hydrogen-bonding molecules: Theoretical insights. *New J Chem*. 2017;41(17):8761-8771. doi:10.1039/c7nj00984d.

9. Duarte LGTA, Germino JC, Braga CDÁ, et al. Photoacidity as a tool to rationalize excited state intramolecular proton transfer reactivity in flavonols. *Photochem Photobiol Sci*. 2018;17(2):231-238. doi:10.1039/c7pp00334j.
10. Chien TC, Dias LG, Arantes GM, et al. 1-(2-Quinolyl)-2-naphthol: A new intra-intermolecular photoacid-photobase molecule. *J Photochem Photobiol A Chem*. 2008;194(1):37-48. doi:10.1016/j.jphotochem.2007.07.012.
11. Rodembusch FS, Leusin FP, Campo LF, Stefani V. Excited state intramolecular proton transfer in amino 2-(2′-hydroxyphenyl)benzazole derivatives: Effects of the solvent and the amino group position. *J Lumin*. 2007;126(2):728-734. doi:10.1016/j.jlumin.2006.11.007.
12. Mei J, Leung NLC, Kwok RTK, Lam JWY, Tang BZ. Aggregation-Induced Emission: Together We Shine, United We Soar! *Chem Rev*. 2015;115(21):11718-11940. doi:10.1021/acs.chemrev.5b00263.
13. Sakakura A, Umemura S, Kondo R, Ishihara K. Dehydrative Cyclization Catalyzed by the Combination of Molybdenum(VI) Oxides and Benzoic Acids: First Synthesis of the Antitumour Substance BE-70016. *Adv Synth Catal*. 2007;349(4-5):551-555. doi:10.1002/adsc.200600550.
14. Tsuda M, Yamakawa M, Oka S, et al. Brasilibactin A, a Cytotoxic Compound from Actinomycete Nocardia brasiliensis. *J Nat Prod*. 2005;68(3):462-464. doi:10.1021/np0496385.

15. McDonald LA, Ireland CM. Patellamide E: a New Cyclic Peptide from the Ascidian Lissoclinum patella. *J Nat Prod*. 1992;55(3):376-379. doi:10.1021/np50081a016.

16. Okujo N, Saito M, Yamamoto S, Yoshida T, Miyoshi S, Shinoda S. Structure of vulnibactin, a new polyamine-containing siderophore from Vibrio vulnificus. *Biometals*. 1994;7(2):109-116. doi:10.1007/BF00140480.

17. Doi T. Synthesis of the Biologically Active Natural Product Cyclodepsipeptides Apratoxin A and Its Analogues. *Chem Pharm Bull*. 2014;62(8):735-743. doi:10.1248/cpb.c14-00268.

18. Wang P, Gong J, Wang B, Zhang M, Wang J. Solubility of Deflazacort in Binary Solvent Mixtures. *J Chem Eng Data*. 2009;54(1):162-164. doi:10.1021/je800790g.

19. Djurendić E, Vujašković D, Sakač M, Ajduković J. Synthesis and biological evaluation of some new 2-oxazoline and salicylic acid derivatives. 2011;2011(ii):83-102.

20. Bansal S, Halve AK. Oxazolines: Their synthesis and biological activity. *Int J Pharm Sci Res*. 2014;5(11):4601-4616. doi:10.13040/IJPSR.0975-8232.5(11).4601-16.

21. Meyers AI, Mihelich ED. The Synthetic Utility of 2-Oxazolines. *Angew Chemie Int Ed English*. 1976;15(5):270-281. doi:10.1002/anie.197602701.

22. Gómez M, Muller G, Rocamora M. Coordination chemistry of oxazoline ligands. *Coord Chem Rev*. 1999;193-195(Supplement C):769-835. doi:https://doi.org/10.1016/S0010-8545(99)00086-7.

23. Hargaden GC, Guiry PJ. Recent Applications of Oxazoline-Containing Ligands in Asymmetric Catalysis. *Chem Rev*. 2009;109(6):2505-2550. doi:10.1021/cr800400z.

24. Lambermont-Thijs HML, van Kuringen HPC, van der Put JPW, Schubert US, Hoogenboom R. Temperature induced solubility transitions of various poly(2-oxazoline)s in ethanol-water solvent mixtures. *Polymers (Basel)*. 2010;2(3):188-199. doi:10.3390/polym2030188.

25. Hoogenboom R. Poly(2-oxazoline)s: A Polymer Class with Numerous Potential Applications. *Angew Chemie Int Ed*. 2009;48(43):7978-7994. doi:10.1002/anie.200901607.

26. Barbeiro CS, Vasconcelos SNS, de Oliveira IM, et al. Suzuki-Miyaura Cross-Coupling Reaction Catalyzed by Palladium Complexes of Hydroxynaphthalene-2-Oxazolines. *ChemistrySelect*. 2017;2(26):8173-8177. doi:10.1002/slct.201701197.

27. Fortman GC, Nolan SP. N-Heterocyclic carbene (NHC) ligands and palladium in homogeneous cross-coupling catalysis: a perfect union. *Chem Soc Rev*. 2011;40(10):5151-5169. doi:10.1039/C1CS15088J.

28. Togni A, Venanzi LM. Nitrogen Donors in Organometallic Chemistry and Homogeneous Catalysis. *Angew Chemie Int Ed English*. 1994;33(5):497-526. doi:10.1002/anie.199404971.

29. Caputo CA, Jones ND. Developments in asymmetric catalysis by metal complexes of chiral chelating nitrogen-donor ligands. *Dalt Trans*. 2007;(41):4627-4640. doi:10.1039/B709283K.

30. Durand J, Milani B. The role of nitrogen-donor ligands in the palladium-catalyzed polyketones synthesis. *Coord Chem Rev*. 2006;250(3):542-560. doi:https://doi.org/10.1016/j.ccr.2005.08.012.

31. Che W, Yu T, Jin D, et al. A simple oxazoline as fluorescent sensor for Zn2 + in

aqueous media. *Inorg Chem Commun*. 2016;69:89-93. doi:https://doi.org/10.1016/j.inoche.2016.03.025.

32. Elliott PIP. Photophysics of metal complexes. *Annu Rep Prog Chem{,} Sect A Inorg Chem*. 2013;109(0):360-378. doi:10.1039/C3IC90030D.

33. Rodriguez-Rodriguez C, Telpoukhovskaia MA, Ali-Torres J, et al. Thioflavin-based molecular probes for application in Alzheimer{'}s disease: from in silico to in vitro models. *Metallomics*. 2015;7(1):83-92. doi:10.1039/C4MT00167B.

34. Zhou Y, Xu Z, Yoon J. Fluorescent and colorimetric chemosensors for detection of nucleotides{,} FAD and NADH: highlighted research during 2004-2010. *Chem Soc Rev*. 2011;40(5):2222-2235. doi:10.1039/C0CS00169D.

35. Mahuteau-Betzer F, Piguel S. Synthesis and evaluation of photophysical properties of Series of π-conjugated oxazole dyes. *Tetrahedron Lett*. 2013;54(24):3188-3193. doi:https://doi.org/10.1016/j.tetlet.2013.04.037.

36. Sahoo SK, Sharma D, Bera RK, Crisponi G, Callan JF. Iron(iii) selective molecular and supramolecular fluorescent probes. *Chem Soc Rev*. 2012;41(21):7195-7227. doi:10.1039/C2CS35152H.

37. Mukhina OA, Kutateladze AG. Oxazolines as Dual-Function Traceless Chromophores and Chiral Auxiliaries: Enantioselective Photoassisted Synthesis of Polyheterocyclic Ketones. *J Am Chem Soc*. 2016;138(7):2110-2113. doi:10.1021/jacs.5b12690.

38. Li C, Xiao P, Fang W-H, Cui G. Excited-state proton transfer induced [4 + 2] and [4 + 4] photocycloaddition reactions of an oxazoline: Mechanism and selectivity. *J Photochem Photobiol A Chem*. 2017. doi:10.1016/j.jphotochem.2017.09.014.

39. Barbeiro CS, Vasconcelos SNS, Zukerman-Schpector J, et al. Chlorinated 2-hydroxynaphthalenoxazolines: Synthesis, Reaction Mechanism and Fluorescence Properties. *ChemistrySelect*. 2016;1(18):5647-5652. doi:10.1002/slct.201601526.

40. Zhao Y, Truhlar DG. The M06 suite of density functionals for main group thermochemistry, thermochemical kinetics, noncovalent interactions, excited states, and transition elements: Two new functionals and systematic testing of four M06-class functionals and 12 other function. *Theor Chem Acc*. 2008;120(1-3):215-241. doi:10.1007/s00214-007-0310-x.

41. Marenich A V., Cramer CJ, Truhlar DG. Universal solvation model based on solute electron density and on a continuum model of the solvent defined by the bulk dielectric constant and atomic surface tensions. *J Phys Chem B*. 2009;113(18):6378-6396. doi:10.1021/jp810292n.

42. Zhao Y, Truhlar DG. Density functionals with broad applicability in chemistry. *Acc Chem Res*. 2008;41(2):157-167. doi:10.1021/ar700111a.

43. Frisch MJ, Trucks GW, Schlegel HB, et al. *Gaussian 09, Revision D. 01; Gaussian*.; 2009. doi:10.1063/1.1672392.

44. Humphrey W, Dalke A, Schulten K. VMD: Visual molecular dynamics. *J Mol Graph*. 1996;14(1):33-38. doi:10.1016/0263-7855(96)00018-5.

45. Zhao J, Ji S, Chen Y, Guo H, Yang P. Excited state intramolecular proton transfer (ESIPT): From principal photophysics to the development of new chromophores and applications in fluorescent molecular probes and luminescent materials. *Phys Chem Chem Phys*. 2012;14(25):8803-8817. doi:10.1039/c2cp23144a.

46. Hao Y, Chen Y. Excited-state intramolecular single and double proton transfer

emission of 2,5-bis(benzoxazol-2-yl)thiophene-3,4-diol. *Dye Pigment*. 2016;129:186-190. doi:10.1016/j.dyepig.2016.03.002.

47. Harris CM, Selinger BK. Acid-base properties of 1-naphthol. Proton-induced fluorescence quenching. *J Phys Chem*. 1980;84(11):1366-1371. doi:10.1021/j100448a016.

48. Dixon SL, Jurs PC. Estimation of pKa for organic oxyacids using calculated atomic charges. *J Comput Chem*. 1993;14(12):1460-1467. doi:10.1002/jcc.540141208.

49. Kirillova TN, Gerasimova MA, Nemtseva E V., Kudryasheva NS. Effect of halogenated fluorescent compounds on bioluminescent reactions. *Anal Bioanal Chem*. 2011;400(2):343-351. doi:10.1007/s00216-011-4716-x.

50. Morrison H, Miller A. An analysis of heavy-atom perturbation of intersystem crossing as a mechanistic tool in photochemistry: Probing for singlet and triplet dominated reactions. *Tetrahedron*. 1981;37(19):3405-3409. doi:https://doi.org/10.1016/S0040-4020(01)92389-0.

51. Koziar JC, Cowan DO. Photochemical heavy-atom effects. *Acc Chem Res*. 1978;11(9):334-341. doi:10.1021/ar50129a003.

52. Catalán J, del Valle JC, Palomar J, Díaz C, de Paz JLG. The Six-Membered Intramolecular Hydrogen Bond Position as a Switch for Inducing an Excited State Intramolecular Proton Transfer (ESIPT) in Esters of *o* -Hydroxynaphthoic Acids. *J Phys Chem A*. 1999;103(50):10921-10934. doi:10.1021/jp992631p.

53. Tolbert LM, Solntsev KM. Excited-State Proton Transfer: From Constrained Systems to “Super” Photoacids to Superfast Proton Transfer. *Acc Chem Res*. 2002;35(1):19-27. doi:10.1021/ar990109f.

54. Mishra H, Maheshwary S, Tripathi HB, Sathyamurthy N. An Experimental and Theoretical Investigation of the Photophysics of 1-Hydroxy-2-naphthoic Acid. *J Phys Chem A*. 2005;109(12):2746-2754. doi:10.1021/jp0461091.

55. Nagaoka SI, Kusunoki J, Fujibuchi T, Hatakenaka S, Mukai K, Nagashima U. Nodal-plane model of the excited-state intramolecular proton transfer of 2-(o-hydroxyaryl)benzazoles. *J Photochem Photobiol A Chem*. 1999;122(3):151-159. doi:10.1016/S1010-6030(99)00025-8.